Study on electronic structure of $CaTiO_3$ by spectroscopic measurements and energy band calculations

1999 J. Phys.: Condens. Matter 11 3535

(http://iopscience.iop.org/0953-8984/11/17/311)

J. Phys.: Condens. Matter **11** (1999) 3535–3545. Printed in the UK PII: S0953-8984(99)98129-8

Study on electronic structure of $CaTiO_3$ by spectroscopic measurements and energy band calculations

K Ueda, H Yanagi, H Hosono and H Kawazoe

Materials and Structures Laboratory, Tokyo Institute of Technology, 4259, Nagatsuta, Midori-ku, Yokohama, 226-8503 Japan

Received 6 October 1998, in final form 3 February 1999

Abstract. The electronic structure of $CaTiO_3$ was experimentally examined by x-ray and ultraviolet photoemission spectroscopy, bremsstrahlung isochromat spectroscopy (BIS) and x-ray absorption spectroscopy. The photoemission spectra and BIS spectra were compared with the partial density of states (PDOS) estimated by an energy band calculation for a fundamental interpretation of the experimental spectra. The calculated PDOS were in reasonable agreement with the experimental energy spectra and the features in the spectra were interpreted by a comparison of the spectra with the PDOS. It was concluded that the top of the valence band mainly consists of O 2p orbitals in non-bonding states and the bottom of the conduction band is composed of Ti 3d orbitals in d-pπ^* anti-bonding states.

1. Introduction

Titanium oxides including alkaline earth perovskites have attracted the attention of many researchers because some titanates are practically used as ferroelectric, electroconductive, photorefractive or photovoltaic materials. It is well known that these applications are based on electrical and optical properties of the materials, and the properties result from their electronic structures or the electronic states of dopants. Therefore, an understanding of the electronic structures of the materials and the electronic states of dopants is fairly important, not only to improve the electrical or optical functions but also to develop other new materials and their new applications.

Rutile, one of the polytypes of titanium dioxides, has been most intensively studied on its electronic structure among the titanates [1–5]. Experimental estimations of its electronic structure by photoemission spectroscopy agree well with theoretical evaluations by energy band calculations. Electrical and optical properties of $SrTiO_3$ and $BaTiO_3$ have also been extensively examined and their electronic structures are relatively well understood [6–19]. However, some inconsistencies have remained between photoemission spectra and theoretical calculations in the materials [11].

In contrast to these titanates, the electronic structure of $CaTiO_3$ has not been studied in detail, although it is one of the alkaline earth titanates with perovskite structure. This is probably because $CaTiO_3$ has not been widely used as a practical material, compared with $SrTiO_3$ and $BaTiO_3$, and there has been less interest in $CaTiO_3$. In addition, the crystal structure of $CaTiO_3$ is distorted from the ideal cubic perovskite structure [20], which makes theoretical approaches rather complicated. However, an understanding of the electronic structures through a series

0953-8984/99/173535+11$19.50

of alkaline earth titanates is significant, from the viewpoint of material science, to pursue the origins of their electrical and optical functions.

We have examined the electrical properties of non-doped and donor-doped $CaTiO_3$ single crystals in order to understand carrier generation and transport mechanisms in the material [21]. The total understanding of the electrical properties will require investigations of two factors: the electronic structure of the material and the electronic states of dopants. Vacuum ultraviolet reflectance and electron energy-loss spectra were measured to examine the electronic structure of $CaTiO_3$ in the previous report [22]. In the present paper, the electronic structure of $CaTiO_3$ have been studied further by normal/inverse photoemission spectroscopy or x-ray absorption spectroscopy, and the spectra were interpreted with the help of an energy band calculation based on the tight-binding method.

2. Experimental details

Single crystals were prepared by the floating zone method using an infrared furnace. H_2-reduced crystals doped with 0.01 at% yttrium were used as samples in the following experiments. The electrical conductivity of the samples was $\sim 10^{-3}$ S cm^{-1} at room temperature.

Photoemission spectroscopy (PES) measurements were carried out in an angle-integrated mode using different excitation energies. In the x-ray photoemission spectroscopy (XPS) measurement, a conventional spectrometer (Perkin-Elmer ESCA model 5500MT) with monochromatic Al Kα radiation (1487 eV) was used. In the ultraviolet photoemission spectroscopy (UPS) measurement, synchrotron radiation with 130 or 150 eV was used on BL-2B1 of UVSOR at the Institute for Molecular Science (IMS). The surface of a sample was slightly etched with an Ar-ion beam in the XPS measurement, or it was scraped by a diamond file at a pressure of $\sim 10^{-9}$ Torr in the UPS measurement. The spectra were obtained under a vacuum of $\sim 10^{-10}$ Torr, and the energy resolution was higher than 0.5 eV. The energy scale of the binding energy was calibrated by use of the Ag 3d level and the C 2s level in the XPS measurement, or by the Fermi level of Au deposited on the sample in the UPS measurement. The peak derived from the C 2s level was observed only before Ar-ion etching in the XPS measurement.

Bremsstrahlung isochromat spectroscopy (BIS) measurements were carried out using our homemade instrument, which detects 9.4 eV photons by a photoelectron multiplier (Hamamatsu: R595) through a SrF_2 window. The BIS is named UV-BIS in the present paper because ultraviolet (UV) light is detected in the measurements. The energy resolution of the BIS spectra was ~ 1 eV and the energy scale was calibrated by the Fermi level of Au deposited on a sample. X-ray absorption spectroscopy (XAS) measurements for Ca $L_{2,3}$ edges, Ti $L_{2,3}$ edges and the O K edge were performed in a total photoelectron yield mode on BL-2B1 of UVSOR. The energy resolution of the measurements was less than 1 eV. In both the BIS and XAS measurements, the surface of a sample was scraped by a diamond file at a pressure of $\sim 10^{-9}$ Torr in the preparation chamber, and the sample was promptly transferred into the analysis chamber. The measurement was carried out under a vacuum of $\sim 10^{-10}$ Torr.

An empirical energy band calculation by the linear combination of atomic orbitals (LCAO) tight-binding method was carried out in order to interpret the experimental energy spectra. Ca 3p, 3d, 4s, Ti 3d, 4s and O 2s, 2p atomic orbitals were used as basis functions. The procedures used in the calculation, such as parametrization, were those proposed by Harrison [23], which were useful for semi-quantitative discussions. In the present simple calculation for a basic interpretation of the experimental spectra, the self-consistent method was not used and

high-order effects such as electron–electron Coulomb repulsion were not calculated. Parameter values adopted in the band calculations of titanates [15–18] and alkali earth perovskites [19], or those proposed by Harrison were used as starting parameters. Changing the parameters independently, their values were properly adjusted to reproduce fundamental experimental results such as an energy gap.

3. Results

3.1. Photoemission spectra

Figure 1 shows PES spectra of $CaTiO_3$ measured using different photon energies. The Fermi level of the spectra was set to zero in the energy scale. Six major bands were observed in the binding energy range up to 40 eV, and they are indexed from A to F. The binding energies of the bands are approximately 5, 7, 11, 22, 26 or 37 eV. The bands A, B and C form the valence band, and the other bands D, E and F form shallow core levels. Referring to the interpretation of the occupied states in $SrTiO_3$ and $BaTiO_3$ by Battye *et al* [11] and the energy levels of atoms [24], the shallow core levels of D, E and F are roughly ascribed to O 2s, Ca 3p and Ti 3p orbitals, respectively. The valence band is expected to consist of O 2p orbitals. This expectation can be supported by enhancement of the valence bands in the UPS spectra, because the ionization cross section of O 2p orbitals increases more rapidly with a decrease in photon energy than those of other orbitals [24]. A theoretical interpretation is necessary for more detailed assignment and will be given in the discussion section.

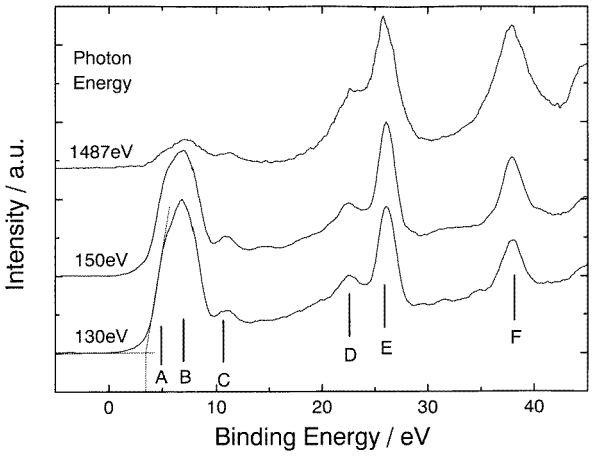

Figure 1. Photoemission spectra of $CaTiO_3$ measured under different excitation energies.

The top edge of the valence band was observed at 3.5 eV below the Fermi level. Since the energy is almost the same as the energy gap which is estimated to be 3.57 eV by the optical transmission measurement [22], it can be concluded that the Fermi level of the sample is located at the bottom of the conduction band. This is consistent with the fact that the sample is an n-type semiconductor owing to the substitution of yttrium ions for calcium ions [21].

3.2. BIS spectrum

Figure 2 shows the BIS spectrum of $CaTiO_3$. The Fermi level (E_F) was fixed at zero on the energy scale. Three broad bands were observed at approximately 2, 7 and 14 eV above the Fermi level, and they are labelled X, Y and Z, respectively. The band X forms the lower part of the conduction band, and the other bands Y and Z form the higher part of the conduction bands or unoccupied bands at high energies. The bandwidth of the Z band is wider than that of the other bands, which probably reflects the fact that the orbitals constituting the band spread over several ions because of its high energy level. The intensity of the BIS spectrum rises from the conduction band edge, indicating that the Fermi level lies at the bottom of the conduction band, which is consistent with the result from the PES measurements.

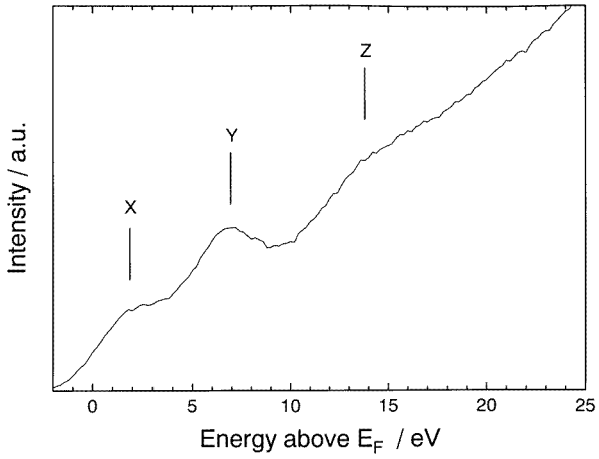

Figure 2. UV-BIS spectrum of $CaTiO_3$ obtained by detecting UV light of 9.4 eV.

3.3. XAS spectra

Figure 3 shows the XAS spectra for the (a) Ca $L_{2,3}$, (b) Ti $L_{2,3}$ and (c) O K edges of $CaTiO_3$. The Ca $L_{2,3}$ edges (figure 3(a)) have two intense bands at 348 and 351 eV and two small bands at 356 and 360 eV. A pair of bands at 348 and 356 eV and another pair of bands at 351 and 360 eV are attributed to the L_3 and L_2 edges, respectively. The Ti $L_{2,3}$ edges (figure 3(b)) also have a pair of intense and small bands for each edge, and the intense unoccupied band is split into two bands under the influence of octahedral crystal fields. Therefore, a pair of intense bands at 458 and 460 eV and a small band at 470 eV are ascribed to the L_3 edge, and the other pair of intense bands at 463 and 465 eV and a small band at 475 eV are ascribed to the L_2 edge. The general features of the XAS spectrum for the Ti $L_{2,3}$ edges in $CaTiO_3$ are similar to those in $SrTiO_3$ reported by Abbate *et al* [25]. Environments around Ti ions which are almost equivalent in the materials are probably responsible for the features. The O K edge (figure 3(c)) has four bands at 531, 534, 536 and 544 eV, and its intensity was lower than those for the Ca $L_{2,3}$ and Ti $L_{2,3}$ edges. This seems to indicate a smaller less contribution of oxygen components to the density of states in the conduction band†.

† The transition probabilities of the Ca 2p, Ti 2p and O 1s orbitals are approximately estimated by their ionization cross sections calculated by Yeh [24]. The ionization cross section, or transition probability, is found to be nearly equivalent in the three transitions from a viewpoint of the one molecule unit, $CaTiO_3$.

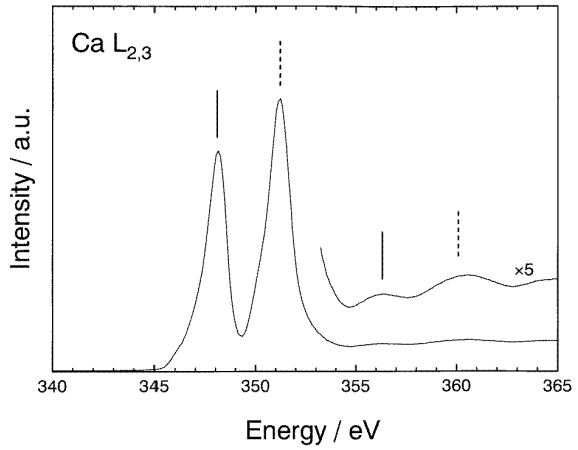

(a)

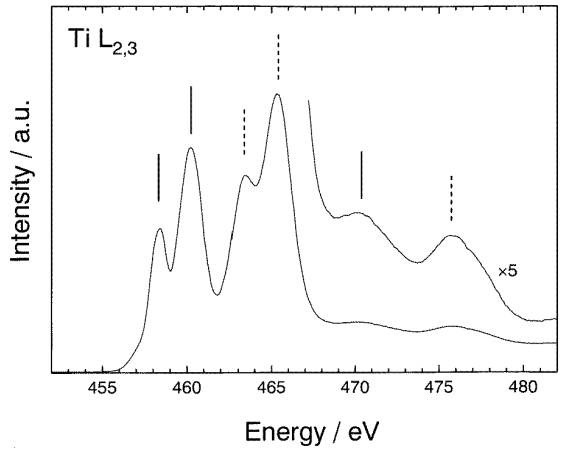

(b)

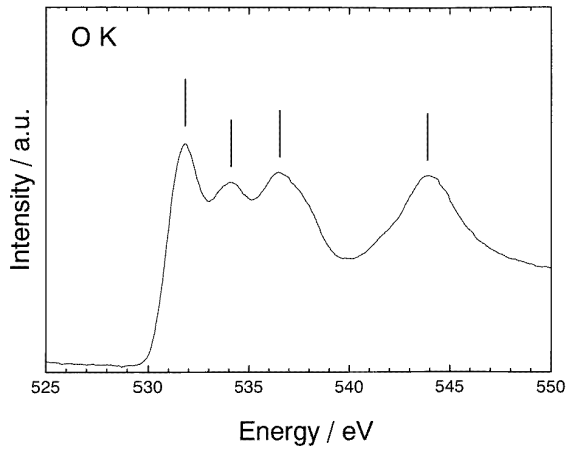

(c)

Figure 3. XAS spectra for (a) Ca $L_{2,3}$, (b) Ti $L_{2,3}$ and (c) O K edges. Bands for the L_3 and L_2 edges are indicated by full and dashed bars, respectively.

3.4. Energy band calculations

Figure 4 shows the energy band structure of $CaTiO_3$ along the symmetry lines of the Brillouin zone (BZ) and the corresponding density of states (DOS). The bottom of the conduction band was set to zero on the energy scale for convenience so that we can compare experimental spectra with the DOS in section 4. The optimized parameters used in the calculations are summarized in table 1. The parameters, $V_{ll'm}$ and V_{ldm}, proposed by Harrison [23] were reduced or gained by multiplying damping factors ξ as follows,

$$V_{ll'm} = \eta_{ll'm}\frac{\hbar^2}{md^2} \times \xi \qquad l \text{ or } l' = \text{s, p} \qquad m = \sigma, \pi, \delta \tag{1}$$

$$V_{ldm} = \eta_{ldm}\frac{\hbar^2 r_d^{3/2}}{md^{7/2}} \times \xi \tag{2}$$

where η, r_d, d and m are a dimensionless coefficient, an atomic-related parameter, the interatomic distance and the mass of the electron, respectively. Some damping factors lead to values of the parameters which are far from the original values. This difference comes from the ionicity of the present material because Harrison obtained the parameters from the theory of and experiments with covalent materials such as silicon.

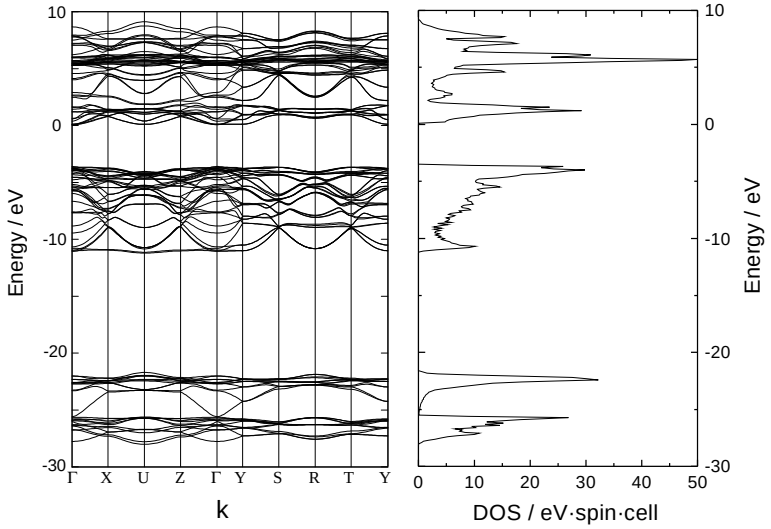

Figure 4. The band structure along the symmetry lines of the BZ (a) and the corresponding DOS of $CaTiO_3$ (b).

Table 1. Energy levels used as diagonal elements in the Hamiltonian matrix and damping factors, ξ, for $V_{ll'm}$ parameters.

	Ca 3p	Ca 3d	Ca 4s	Ti 3d	Ti 4s	O 2s	O 2p	
H_{ii} (eV)	−37.18	−6.32	−5.42	−11.49	−7.36	−34.36	−16.09	
	Ca–Ti	Ca–O	O–O	Ti–O	Ca–O(d-pσ)	Ca–O(d-pπ)	Ti–O(d-pσ)	Ti–O(d-pπ)
ξ	0.20	0.20	0.15	0.50	0.40	1.50	1.30	1.60

Since the crystal structure of $CaTiO_3$ is of distorted perovskite type and four molecular units are in the unit cell, the number of electronic states at a k point is four times more than that of $SrTiO_3$ with an ideal cubic perovskite structure. Therefore, the band structure along the symmetry lines is fairly complex and discussion of the band diagram is fairly difficult. In addition, no experimental information about k space, such as the angle-resolved photoemission spectra, is available so far. Accordingly, the following discussions will concern primarily the DOS rather than the band structure along the symmetry lines.

4. Discussion

4.1. Band assignments in PES and BIS spectra

Figure 5 shows the DOS and partial density of states (PDOS) of $CaTiO_3$ estimated by a tight-binding band calculation with its PES (UPS) and BIS spectra. It should be noted that there is no relationship between the PES and BIS spectra in their relative intensities. The Fermi levels in the experimental spectra and the bottom of the conduction band in the DOS and PDOS are set to zero on the energy scale. Since sample surfaces are rough on an atomic scale after filing and their detailed states are unknown, surface effects on the spectra will be tentatively neglected in the present discussion. An energy gap was observed between the valence band edge in the PES spectrum and the conduction band edge in the BIS spectrum, and its magnitude (∼3 eV) is close to the value (3.57 eV) estimated by the optical transmission measurement. In the following discussion, several bands observed in each spectrum are assigned by a comparison with the PDOS.

In the occupied states shown in the PES spectrum, the bands D and E are mainly composed of O 2s and Ca 3p orbitals, respectively, with some mixing between them. The O 2p orbitals

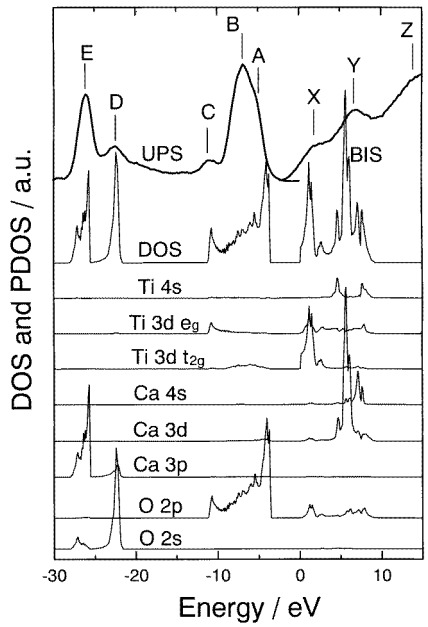

Figure 5. The DOS and the PDOS of $CaTiO_3$ with UPS spectrum ($E_{ex} = 130$ eV) and BIS spectrum ($h\nu = 9.4$ eV). DOS and PDOS, thin full curves; UPS and BIS spectra, thick full curves.

are dominant in the valence band. Band A is exclusively composed of O 2p orbitals, showing the non-bonding states at the top of the valence band. Band B includes a small density of Ti 3d t_{2g} component in addition to the O 2p component, indicating the formation of d-pπ bonds between them in the middle of the valence band. A relatively large DOS of the Ti 3d e_g orbitals is found in band C as well as that of O 2p orbitals. This large hybridization is characteristic of the band, and band C is interpreted as the strong d-pσ bonding states between Ti 3d e_g and O 2p orbitals†.

In the unoccupied states observed in the BIS spectrum, the band X mainly consists of Ti 3d orbitals, especially Ti 3d t_{2g} orbitals. Since O 2p orbitals form some density in the bottom of the conduction band in addition to the Ti 3d t_{2g} orbitals, the bottom of the conduction band can be interpreted as d-pπ^* anti-bonding states between Ti 3d t_{2g} and O 2p orbitals. The band derived from the Ti 3d e_g orbitals spreads above the Ti 3d t_{2g} band according to the PDOS, showing a relatively wide bandwidth. The band can be regarded as the d-pσ^* anti-bonding states between Ti 3d e_g and O 2p orbitals, which are paired with the d-pσ bonding states in the valence states. However, the band does not appear clearly in the BIS spectrum because of its low intensity. The band derived from Ca 3d is located in an energy range higher by $\sim$6 eV than the bottom of the conduction band and these orbitals are expected to be responsible for the band Y. The Ca 4s or Ti 4s orbitals form their bands in an energy range a few eV higher than the Ca 3d band, although they are not clearly observed in the BIS spectrum. The band calculation did not include orbitals with higher energy than 10 eV above the Fermi level. Therefore, the origin of the band Z cannot be determined in the present study.

The width of the conduction band of $CaTiO_3$ is not large in comparison with those of the oxides such as In_2O_3 and SnO_2 in which the conduction bands are formed by s^0 orbitals of the cations [26]. Since electron transport properties of the materials are closely related to the bandwidth of the conduction band, it seems to be reasonable that the electron mobility of $CaTiO_3$, $\sim$3 $cm^2\ V^{-1}\ s^{-1}$ [21], is smaller than that of SnO_2, $\sim$200 $cm^2\ V^{-1}\ s^{-1}$ [27] at room temperature‡ and small polarons tend to be formed in $CaTiO_3$. The structures in the BIS spectrum of $CaTiO_3$ were similar to that in the UV-BIS and x-ray-BIS spectra of $SrTiO_3$ reported by Reihl *et al* [13] and Tezuka *et al* [14]. This similarity probably originates from the analogous crystal structure between $CaTiO_3$ and $SrTiO_3$, even if $CaTiO_3$ has an orthorhombic distortion from an ideal cubic perovskite structure. The electronic structure of the conduction bands plays an important role in the electronic conduction of n-type semiconductors. It seems to be reasonable to observe similar electron transport properties among the alkaline earth titanates [21, 29, 30], because the Ti 3d band primarily forms their conduction bands.

4.2. Comparison of XAS spectra with PDOS and BIS spectrum

XAS spectra generally reflect intra-atomic excitations and the features of the spectra are determined by ions or elements in the materials. Provided that the bandwidth of the core levels or initial states in each transition is negligibly small compared with that of the conduction band, the structure of the spectra is substantially determined by the structure of the final

† A similar peak is found in $SrTiO_3$ UPS spectra and it is assigned to C 2s emission [13]. However, no correlation between the intensity of the peak C and that of C 1s emission was observed in the present examination. Although the possibility of another surface state may be left for the peak C, it was tentatively assigned to d-pσ bonding between the Ti 3d and O 2p orbitals by the result of band calculations with a strong interaction between the two orbitals.

‡ The temperature dependence of mobility or the value of mobility at room temperature is analogous between $CaTiO_3$ and $SrTiO_3$. Since the effective masses of the conduction electrons in $SrTiO_3$ and SnO_2 are estimated to be $\sim 20m_e$ and $\sim 0.3m_e$ (m_e denotes an electron mass), respectively, the comparison in order of magnitude would be adequate in a first approximation [6, 16, 28].

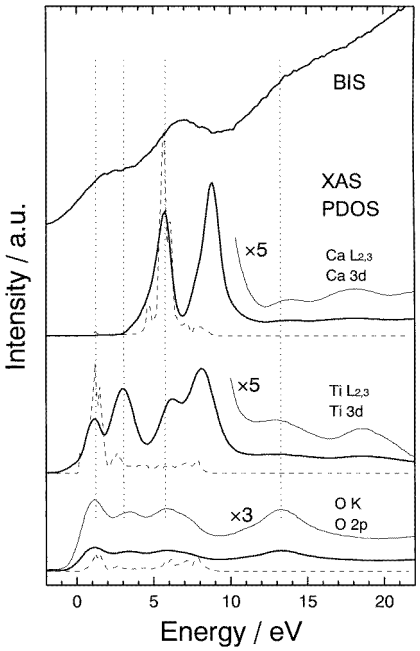

Figure 6. Comparison of XAS spectra (full curves) with PDOS (dashed curves) and the BIS spectrum. The energies of four distinct bands in the XAS spectra are indicated by vertical dotted lines.

states, that is, the PDOS of the conduction band [31]. Therefore, it is supposed that XAS spectra generally provide the PDOS of conduction bands for each element, while BIS spectra provide the total DOS. Accurate analysis of XAS spectra requires the calculation of the dipole matrix elements as studied by de Groot *et al* [32, 33]. However, the calculation of the matrix elements is much more advanced and complicated than the calculation by the tight-binding method. In the present discussion, we confine ourselves to a general and fundamental interpretation of experimental spectra, and XAS spectra were simply compared with PDOS under the consideration of selection rules.

According to the selection rule for electric dipole transitions in atoms, transitions to s or d orbitals are allowed for $L_{2,3}$ edges and transitions to p orbitals are permitted for a K edge. Therefore, it is expected that the Ca $L_{2,3}$ edges show the transitions to the Ca 4s and 3d bands, the Ti $L_{2,3}$ edges reflect the transitions to the Ti 3d and 4s bands, and the O K edge shows the transition to an O 2p band in the anti-bonding states. On the basis of this assumption, the XAS spectra were compared with the PDOS estimated by an energy band calculation. In the comparison of the XAS spectra for Ca and Ti edges, the PDOS of Ca 3d and Ti 3d orbitals were tentatively selected as the corresponding PDOS.

Figure 6 shows the comparison of the XAS spectra with the corresponding PDOS obtained by a tight-binding band calculation and the BIS spectrum. Since there is no quantitative relationship between the XAS spectra and the PDOS in their intensities, the intensities are adjusted arbitrarily. However, the relative intensities of the spectra between elements are not changed within the XAS spectra or PDOS. The bottom of the conduction band is set to zero on the energy scale for the PDOS, as for figure 5. The energy scale for the XAS spectra is taken so that they fit the corresponding PDOS. On adjusting the energy scale, only the bands for the L_3 edge are noted in the Ca or Ti $L_{2,3}$ edges.

The XAS spectrum for the Ca edge simply shows a single intense band similar to the Ca 3d PDOS. However, small structures are not seen in the XAS spectrum. Although the energy splitting of the Ti 3d band by crystal fields is observed in its XAS spectrum and PDOS, the intensity of the split bands is rather different between the XAS spectrum and the PDOS. The deviation in the intensity is due to the neglect of the calculation of the dipole matrix elements. The energies of four bands in the O K edge agree with those of the bands derived from the cations in the XAS spectra indicating the anti-bonding states of O 2p bands. There may be some contribution of Ca 4s and Ti 4s bands to the structure of the conduction band. However, no remarkable bands originating from these bands were observed in the XAS spectra for the Ca and Ti $L_{2,3}$ edges nor in the BIS spectrum. Because transitions to 3d states usually dominate over transitions to 4s states [32, 33], the contribution of Ca 4s and Ti 4s bands to the structure of the conduction band is not obvious in the present analysis.

It is expected that the BIS spectrum reflects some features of the XAS spectra because these two spectra are considered to express the total and partial DOS, respectively. Although small energy deviations of the band energies between the spectra were observed, probably due to thermal or instrumental effects, it would not largely influence the following basic interpretation of the spectra. Four distinct bands constituting unoccupied states were observed in a series of the XAS spectra and they agreed with bands in the BIS spectrum: a pair of Ti 3d bands at 1 and 3 eV in the XAS spectra corresponds to the X band at 2 eV in the BIS spectrum, and a Ca 3d band at 6 eV corresponds to the Y band at 7 eV. Moreover, the unknown Z band at 13–14 eV in the BIS spectrum was observed in all XAS spectra. However, it should be noted, on interpreting the Z band, that XAS spectra may include multielectronic excitations which result in satellite bands as reported by van der Laan [34] or Okada and Kotani [35]. Although the assignment of the high-energy bands at 13–14 eV still remains, it was understood that a combination of XAS and BIS spectra provides useful information about the conduction bands of materials.

5. Conclusion

The electronic structure of $CaTiO_3$ was analysed experimentally and theoretically. Information concerning the occupied states, both for the valence band and shallow core levels, was obtained by XPS and UPS measurements, while information concerning the unoccupied states was acquired by BIS and XAS measurements. The experimental spectra were interpreted by a comparison with PDOS estimated by a tight-binding energy band calculation. It was concluded that the top of the valence band is mainly composed of the O 2p orbitals in non-bonding states and the lower part of the valence band is formed by bonding states between the Ti 3d and O 2p orbitals. Two shallow core levels, which are located at 22 and 26 eV in binding energy, are assigned to the O 2s and Ca 3p orbitals, respectively. The conduction band mainly consists of Ti 3d and Ca 3d bands with a small contribution of the O 2p anti-bonding bands: a band at 2 eV above the Fermi level in the BIS spectrum corresponds to a Ti 3d band and another band at 7 eV in the BIS spectrum corresponds to a Ca 3d band. A band at 13–4 eV was observed in both BIS and XAS measurements, but its origin is unknown so far.

Although the approximation level of the present band calculations, including DOS calculations, was not sufficiently high, the results of the calculations showed a reasonable agreement with the experimental spectra which were obtained independently. Combination of normal and inverse photoemission spectroscopy enabled us to observe the energy structure of $CaTiO_3$ in the wide energy range over the Fermi energy. The positions of the Fermi energy obtained by this spectroscopy were consistent with each other, indicating that the samples used are n-type electrical conductive with $\sim$3.5 eV energy gap. The structure in the O K edge

XAS spectrum was experimentally interpreted as anti-bonding states of the O 2p orbitals by a comparison with Ca and Ti $L_{2,3}$ edge XAS spectra. From a comparison between the XAS and the BIS spectra it was found that information obtained by XAS spectroscopy is complementary to that obtained by inverse photoemission spectroscopy.

Acknowledgments

We would like to thank Dr Kameshima of Tokyo Institute of Technology for the support in the XPS measurement. This work was supported in part by the fund from the Murata Science Foundation.

References

[1] Cardona M and Harbeke G 1965 *Phys. Rev.* **137** A1467
[2] Vos K and Krusemeyer H J 1977 *J. Phys. C: Solid State Phys.* **10** 3893
[3] Vos K 1977 *J. Phys. C: Solid State Phys.* **10** 3917
[4] Glassford K M and Chelikowsky J R 1992 *Phys. Rev.* B **46** 1284
[5] Mo S D and Ching W Y 1995 *Phys. Rev.* B **51** 13 023
[6] Cardona M 1965 *Phys. Rev.* A **140** 651
[7] Bauerle D, Braun W, Saile V, Spussel G and Koch E E 1978 *Z. Phys.* B **29** 179
[8] Frova A and Boddy P J 1967 *Phys. Rev.* **153** 606
[9] Frova A and Boddy P J 1966 *Phys. Rev. Lett.* **16** 688
[10] Yacoby Y and Naveh O 1973 *Phys. Rev.* B **7** 3991
[11] Battye F L, Hochst H and Goldmann A 1976 *Solid State Commun.* **19** 269
[12] Haruyama Y, Kodaira S, Aiura Y, Bando H, Nishihara Y, Maruyama T, Shakisara Y and Kato H 1996 *Phys. Rev.* B **53** 8032
[13] Reihl B, Bednorz J G, Muller K A, Jugnet Y, Landgren G and Morar J F 1984 *Phys. Rev.* B **30** 803
[14] Tezuka Y, Shin S and Ishii T 1994 *J. Phys. Soc. Japan* **63** 347
[15] Mattheiss L F 1972 *Phys. Rev.* B **6** 4718
[16] Kahn A H and Leyendecker A J 1964 *Phys. Rev.* **135** A1321
[17] Soules T F, Kelly E J, Vaught D M and Richardson J W 1972 *Phys. Rev.* B **6** 1519
[18] Pertosa P and Michel-Calendini F M 1978 *Phys. Rev.* B **17** 2011
[19] Takegahara K 1994 *J. Electron Spectrosc. Relat. Phenom.* **66** 303
[20] Sasaki S, Prewitt C T and Bass J D 1987 *Acta Crystallogr.* C **43** 1668
[21] Ueda K, Yanagi H, Hosono H and Kawazoe H 1997 *Phys. Rev.* B **56** 12 998
[22] Ueda K, Yanagi H, Noshiro R, Hosono H and Kawazoe H 1998 *J. Phys.: Condens. Matter* **10** 3669
[23] Harrison W A 1980 *Electronic Structure and the Properties of Solids* (San Francisco, CA: W H Freeman) ch 4
[24] Yeh J J and Lindau I 1985 *At. Data Nucl. Data Tables* **32** 1
[25] Abbate M *et al* 1991 *Phys. Rev.* B **55** 5419
[26] Robertson J 1979 *J. Phys. C: Solid State Phys.* **12** 4767
[27] Fonstad C G and Rediker R H 1971 *J. Appl. Phys.* **42** 2911
[28] Button K J *et al* 1971 *Phys. Rev.* B **4** 4539
[29] Frederikse H P R, Thurber W R and Hosler W R 1964 *Phys. Rev.* **134** A442
[30] Tufte O N and Chapman P W 1967 *Phys. Rev.* **155** 796
[31] Douillard L, Jollet F, Bellin C, Gautier M and Duraud J P 1994 *J. Phys.: Condens. Matter* **6** 5039
[32] de Groot F M F, Fuggle J C, Thole B T and Sawatzky G T 1990 *Phys. Rev.* **42** 5459
[33] de Groot F M F, Fuggle J C, Thole B T and Sawatzky G A 1990 *Phys. Rev.* **41** 928
[34] van der Laan G 1990 *Phys. Rev.* B **41** 12 366
[35] Okada K and Kotani A 1993 *J. Electron Spectrosc. Relat. Phenom.* **62** 131